QRS-T angle as a biomarker for LBBB strict diagnose

Beatriz del Cisne Macas Ordóñez[1,2], José Manuel Ferrández-Vicente[3], and María Paula Bonomini[1,2]

[1] Instituto Argentino de Matemática "Alberto P. Calderón" (IAM), CONICET, Argentina. paula.bonomini@conicet.gov.ar
[2] Instituto de Ingeniería Biomédica (IIBM), Fac. de Ingeniería, Universidad de Buenos Aires. bmacas.ext@fi.uba.ar
[3] Dpto. Electrónica, Tecnología de Computadoras y Proyectos, Univ. Politécnica de Cartagena, Cartagena, Spain. jm.ferrandez@upct.es

Abstract. Currently, the diagnosis of left bundle branch block (LBBB) is based on the duration of the QRS complexes. However, aberrant QRS complexes, characteristic of LBBB, obscure the delineation process, and therefore, unreliable QRS durations are produced, due to erratic fiducial points. To overcome this flaw, we propose the QRS-T angle as an alternative LBBB biomarker, which is independent of QRS duration. A subset of heart failure patients with and without LBBB was compared to a set of healthy patients, all obtained from the Telemetric and ECG Holter Warehouse Project. The methodology included signal filtering, construction of QRS and T loops and obtention of depolarization and repolarization dominant vectors. Finally, the QRS-T angle in the different 2D and 3D spaces were calculated. Results show that patients with LBBB have much larger QRS-T angles compared to Controls. Moreover, QRS-T angles in the XY plane and the XYZ volume were the markers that best separated LBBB from intact conduction patients, with accuracies of 100% and 96.9%, respectively. These results set the foundations to further investigate the QRS-T angle as a biomarker for the diagnosis of left bundle branch block.

Keywords: QRS-T angle · Left bundle branch block (LBBB) · vectorcardiogram

1 Introduction

Electrical stimulation has provided several solutions in the biomedical field, including sensory restoration and cardiac dysfunction [12, 11, 21]. Particularly in cardiology, the first pacemaker was implanted in Sweden in 1957, and since then, the career of implantable pacemakers has not stopped. Normally, pacing catheters are placed at the tip of the right ventricle (apex) to ensure the mechanical stability that chronic pacing requires. However, evidence on the deleterious effects of pacing in the apex has recently been generated [2]. For this reason, the search for alternative cardiac pacing sites has intensified in recent years,

from which His bundle pacing (septal pacing) has emerged as the most physiological and convenient alternative. Over time, mechanically stable sheaths and catheters were achieved that allowed chronic septal stimulation schemes [1]. In this context, the study of intraventricular dyssynchrony for the selection of the optimal pacing site became vitally important, since the interventricular septum is relatively extensive [20]. In addition, the evaluation of cardiac dyssynchrony today determines the selection of those patients who would potentially benefit from biventricular pacing therapies, such as cardiac resynchronization therapy (CRT) [7]. Currently, QRS duration is the only electrocardiographic parameter of cardiac dyssynchrony, so only those patients with a wide QRS (>120 ms) are recommended for CRT (Dickstein et al., 2008). Paradoxically, 43% of patients with heart failure and narrow QRS (<120 ms) have mechanical dyssynchrony on echocardiography. Furthermore, when dyssynchrony is well documented by all echocardiographic methods, response to therapy tends to be favorable regardless of QRS duration [8].
Recently, a new approach has emerged, aiming to evaluate CRT clinical outcome based on LBBB diagnosis. Many reports focus on reducing CRT non-responders rate by improving its indication. Since most LBBB patients are likely to receive CRT, then, refining LBBB diagnosis would have a positive impact on the amount of patients that would effectively benefit from CRT [17]. In this piece of work, we computed the QRS-T angles on LBBB patients and compared them with those from native conduction subjects in different spaces.

2 Materials and Methods

Study population The data were provided by the ECG Telemetry and Holter ECG Warehouse (THEW), two databases are the subject of the present study, one containing the records of healthy subjects (Health group) and a second database containing the records of patients with left bundle-branch block (LBBB group). The database E-OTH-12-0602-024 [18], contains 602 recordings of heart failure patients included in the Multi-center Autonomic Defibrillator Implantation (MADIT-CRT) clinical trial, publicly available at the THEW project, from University of Rochester (Rochester, NY). The 12-lead high-resolution ECGs were recorded before CRT implantation using 24-hours Holter recorders (H12+, Mortara Instruments, Milwaukee, WI, USA) with Mason-Likar lead configuration (the Mortara system provides 10 electrodes and records 8-lead signals [I, II, V_1-V_6] the other 4 leads are calculated). The first 20-minute ECG signals were recorded while the patients were in a supine position. The sampling frequency was 1 kHz and amplitude resolution 3.75 microVolts. The database E-HOL-03-0202-003 (Intercity Digital Electrocardiogram Alliance – IDEAL)[22],contains 202 recordings of healthy individuals captured from Holter recordings (SpaceLab-Burdick Inc.) of around 24 hours. The ECG signals have a sampling frequency of 200 Hz, an amplitude resolution of 10µV, and have been captured using a three pseudo-orthogonal leads configuration (x, y, z).

Preprocessing In the preprocessing stage, a fourth-order Butterworth band-pass filter was used in the range of 0.5-40 Hz, in order to remove baseline drift and high-frequency noise. For the LBBB group, VCG records were reconstructed by means of the inverse Dower matrix as shown in Table 1. This transformation poses the orthogonal leads, *x*,*y*,*z*, as linear combinations of the eight linearly independent ECG leads. It is worth mentioning that this transform only applied to the LBBB group, since recordings from the Control group were already obtained from the Frank orthogonal lead system.

Lead	V1	V2	V3	V4	V5	V6	I	II
X	-0.172	-0.074	0.122	0.231	0.239	0.194	0.156	-0.010
Y	0.057	-0.019	-0.106	-0.022	0.041	0.048	-0.227	0.887
Z	-0.229	-0.310	-0.246	-0.063	0.055	0.108	0.022	0.102

Table 1: Transformation matrix for Inverse Dower transformation (IDT).

The control and LBBB signals were delineated by means of a wavelet-based algorithm using the WT-delineator library in Python.[15]. The delineation algorithm detects the onset and offset of the QRS and T-wave, from which the QRS and T loops were constructed.
It is important to note that patients from the LBBB group come from the MADIT trial, including all kind of heart failure patients. With the help of independent physicians, all 602 heart failure patients were classified into three classes: "strict LBBB", "not strict LBBB" and "not LBBB". Therefore, from the E-OTH-12-0602-024 database, only the first 200 records were utilized in order to balance the data with the Control group (n = 200). Afterwards, from the first 200 delineated records, only those with "strict LBBB" and aceptable fidutial points were preserved, keeping 47 electrocardiographic records. Finally, 60 VCG records from the Control group were obtained.

QRS-T Angles QRS segments were obtained by applying a window that spanned between the median of the QRS onsets and offsets of all beats in the recording. This window was centered on the QRS peak of every QRS complex. Afterwards, an ensemble was constructed with the above QRS segments and averaged in order to obtain a QRS template on every vectorcardiographic lead *x*,*y*,*z*. A similar procedure was accomplished in order to derive a T-wave template. Following obtention of the QRS and T templates, the vectorcardiographic loops were constructed and aligned to the same origin, and dominant vectors defined as the maxima euclidean norm progressing between the onset and offset of the QRS and T loops in each of the following coordinate systems *xy*, *xz*, *yz* and *xyz*, as shown in equation 1 for the XY plane case:

$$opt = \arg\max_i \left\{ d[i] = \sqrt{(x[i] - x[0])^2 + (y[i] - y[0])^2} \right\}, 0 <= i <= t_{off} \quad (1)$$

Where $x[0]$ and $y[0]$ are the QRS and T loop origins and t_{off} denotes the duration of the QRS or the T-wave templates, respectively. Dominant depolarization and repolarization vectors were then defined as $\mathbf{QRS}_{opt}/\mathbf{T}_{opt} = \{x[opt], y[opt]\}$. Once the QRS and T dominant vectors were determined, the angle between both was computed for every coordinate system as follows:

$$\theta_{QRS-T} = \left\{ \frac{180}{pi} \right\} \arccos \frac{< \mathbf{QRS}_{opt}, \mathbf{T}_{opt} >}{|\mathbf{QRS}_{opt}| * |\mathbf{T}_{opt}|} \tag{2}$$

where $< \mathbf{QRS}_{opt}, \mathbf{T}_{opt} >$ denotes the inner product of the dominant vectors and $|\mathbf{QRS}_{opt}|$, $|\mathbf{T}_{opt}|$ their L_2 norms.

3 Statistical analysis

Descriptive data are presented as mean ± SD. Normality was assessed by means of the Shapiro-Wilks test. For comparison between two independent groups, the Mann-Whitney U Test was utilized.
To test the informative power of angles in the different planes, we constructed a simple Tree decision algorithm with 13 nodes and tested it on every coordinate space XY, XZ, YZ and XYZ. Data splitting was carried out as follows: 70% (n= 75) of the data was used for the training and remaining 30% (n = 32) for testing. The classification scheme was binary "LBBB" vs "not LBBB", where "not LBBB" gathered together "not strict LBBB" and "not LBBB" instances. In order to reduce the effect of overfitting, a cross-validation scheme was set to 5 folds.

4 Results

4.1 QRS-T angles

Figure 1 represents the electrical currents within the heart during a cardiac cycle in terms of its vectorcardiogram, showing the ventricular contraction (QRS complex forming the large loop) and the relaxation phase (T waves including the small loop) for representative Control and LBBB patients. Notice that in the LBBB case, a widening of the QRS complex as well as an inversion in the T-wave can be confirmed, opposite to the Control case, where narrow and consistent QRS and T-waves appear.

In analogy, Figure 2 shows the loops generated from VCG for a healthy and LBBB patient. Notice in the LBBB patient, that T-wave inversion is reflected in a repolarization loop pointing to the opposite side than the depolarization loop. This produces enlarged QRS-T angles, in average greater than 90°. Note also the widened QRS complex for the pathological case, which in turn produces QRS loops with higher energy, as can be appreciated in Fig. 2. Finally, note the twisted morphology of the depolarization loop in the LBBB case, evidencing a much more intrincated electrical path, in contrast with those with native conduction (Controls), the cardiac electrical vector shows a clearly defined trajectory.

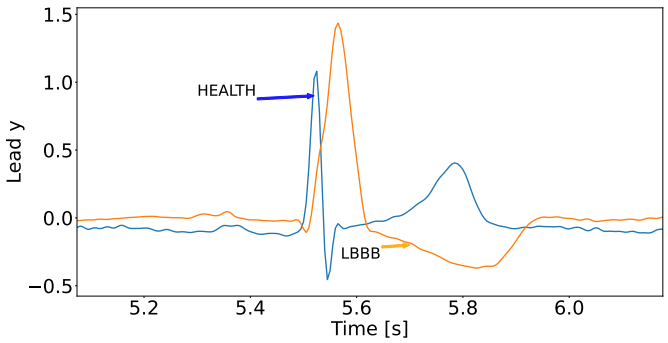

Fig. 1: VCG Control Group/ LBBB Group

Figure 3 illustrates the average QRS-T angles in the different planes, as well as in the XYZ volume, resulting in angles under 70 °for the Control group. This result is confirmed by Cortez y Schlegel in his study [9] where the Dower-related reconstruction results in a spatial QRS-T angle of 66°to 81°.

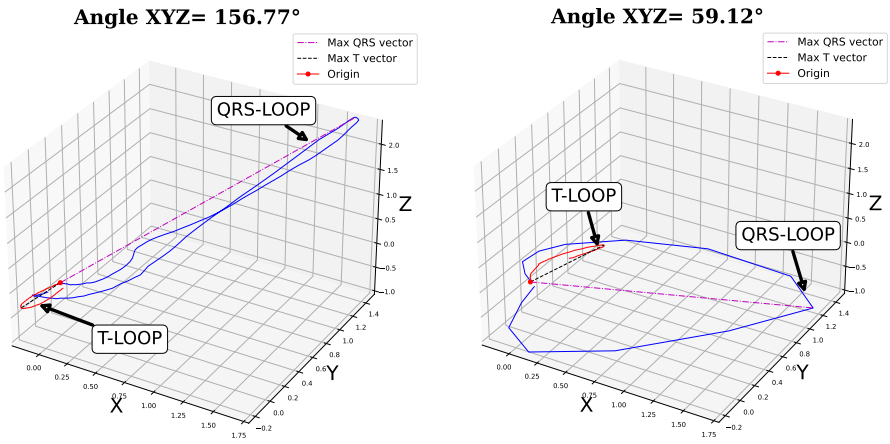

(a) (b)

Fig. 2: VCG angles: (**a**) LBBB Group. (**b**) Health Group

On the contrary, in the case of subjects with left bundle branch block, the median QRS-T angles were greater than 146 °in every 2D and 3D representations. Note that QRS-T angles resulted statistically significant in all four analyzed spaces according to the Mann-Whitney U test, with p-values lesser than 0.05.

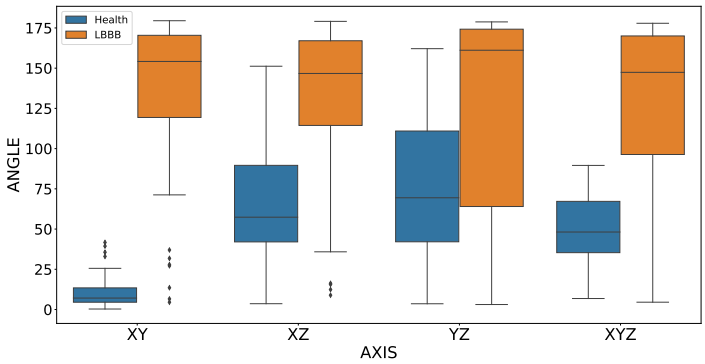

Fig. 3: Intercuartile distribution of QRS-T angles in different coordinate systems for the LBBB and Control group. QRS-T in the LBBB group was significantly increased with respect to the Control group (Mann-Whitney U test, $p < 0.05$) in all analyzed spaces.

4.2 Classification results

Figure 4 shows the confusion matrices obtained for the test sets on every constructed model, each related to a different space. Notice that each model represents a Tree algorithm with 13 nodes, fed by the angles in one out of four spaces analyzed in this piece of work: XY, ZY and XZ planes and the XYZ volume. Surrounding the confusion matrices there are the performance metrics. Bottom corner: accuracy, Top right: precision for Controls, Top middle: precision for LBBB, Bottom left: specificity for "LBBB" class, Bottom middle: sensitivity for "LBBB" class. Notice that the XY plane turned out to be the most informative when separating LBBB from Controls (accuracy=100%), followed by the volume XYZ (accuracy=96.9%).

5 Discussion and conclusions

In this study, an algorithm using the WT-delineator library in Python was used. The wavelet-based model introduced by martinez et all [16], has the highest performance in both sensitivity and accuracy (Se=99.8% and P+=99.86%), which is why it was chosen for the present study. It is important to note that despite the good sensitivity of the delineator used, a manual validation of the detected fidutial points was necessary due to the nature of the ECG recordings of patients with LBBB, where the detection of fidutial points is severely hampered by aberrant QRS morphologies.

The concept of the spatial QRS-T angle has been known for a long time [10] and it has recently regained interest as an independent predictor of cardiac death [14]. It has also been shown that the enlarged QRS-T angle predicts ventricular

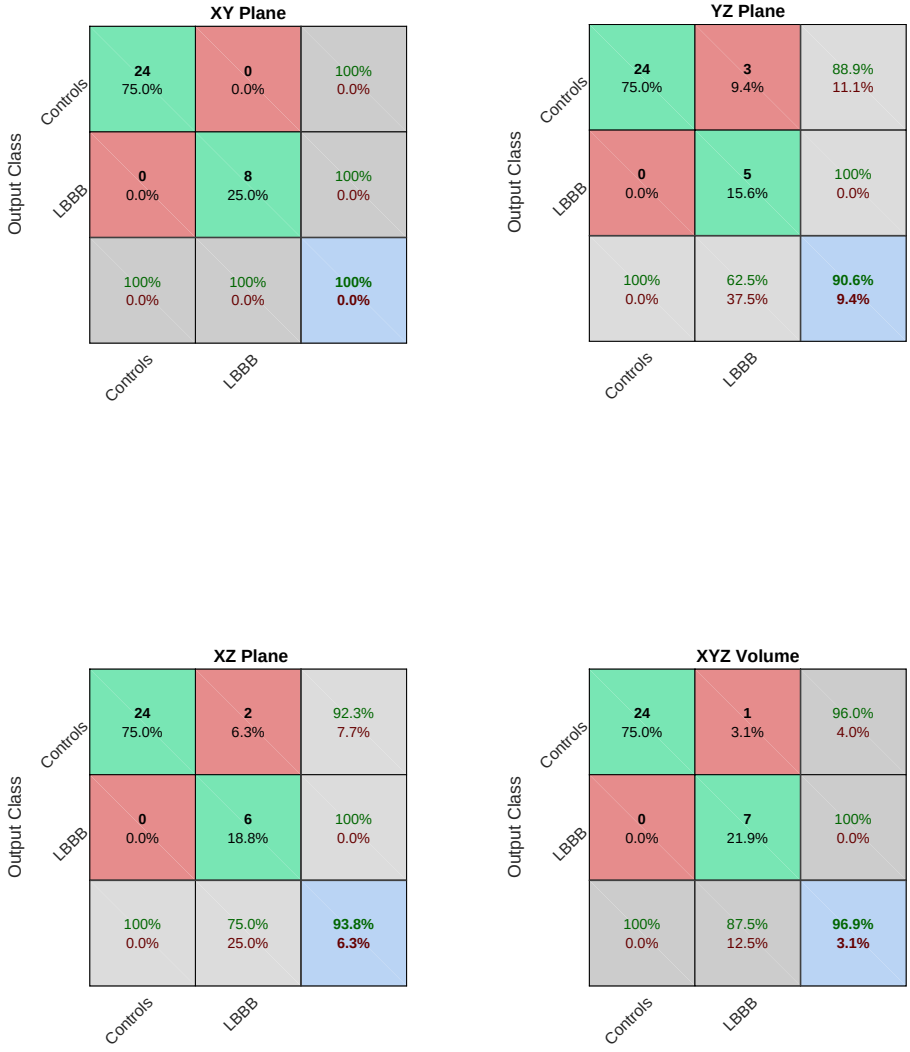

Fig. 4: Confusion matrices for the 4 models analyzed, each one related to a single feature or angles in a plane (or volume). Surrounding the 2x2 confusion matrix there are the performance metrics. Bottom corner: accuracy, Top right: precision for Controls, Top middle: precision for LBBB, Bottom left: specificity for "LBBB" class, Bottom middle: sensitivity for "LBBB" class.

arrhythmias, since narrow spatial angle were associated with a lower risk of ventricular arrhythmias [13]. The main objective of the present study is to set the basis for the measurement of QRS-T angles with an LBBB-diagnosis purpose.
In a normal myocardium, the QRS and T-vector loops point in the same spatial direction, but with changes in ventricular depolarization and repolarization, the vectors point in opposite spatial directions [19]. This is specially true in LBBB, and one of the foundations in postulating the QRS-T angle as a biomarker for LBBB. In this case, we set the distribution values for both populations in different spaces, analyzing either planar and spatial QRS-T angles. We postulate that the VCG is a more compact space that will describe with minimum dimensions the trajectory of the cardiac electrical activity. However, more posibilities should be analyzed, such as preferential planes obtained by PCA, for instance, in order to infer which representation suits best the problem, as in [3, 4].
Many efforts have been done to quantify cardiac dyssynchrony in the last decade. Our group pioneered on septal stimulation [21] and proposed a no invasive models to predict electrical activation of the left ventricle measured invasively [6, 2, 5]. However, these models, since they were based on electrophysiologic studies, accounted for few data, generally under 50 patients. This opportunity, the THEW project allowed us to analyze a higher amount of data in order to have more realistic results. Even though the study presented in this work is a foundational analysis, further studies should improve the delineation process of LBBB patients in order to complete the analysis for the entire dataset, and be able to separate not strict from strict from not LBBB. Results herein encourage such further efforts.

References

1. Barba-Pichardo, R., Moriña-Vázquez, P., Fernández-Gómez, J., Venegas-Gamero, J., Herrera-Carranza, M.: Permanent his-bundle pacing: seeking physiological ventricular pacing. Europace **12**, 527–533 (2010)
2. Bonomini, M.P., Ortega, D.F., Barja, L.D., Mangani, N.A., Paolucci, A., Logarzo, E.: Electrical approach to improve left ventricular activation during right ventricle stimulation. Medicina (Buenos Aires) **77**, 7–12 (2017)
3. Bonomini, M.P., Corizzo, S.J., Laguna, P., Arini, P.D.: 2d ecg differences in frontal vs preferential planes inpatients referred for percutaneous transluminal coronary angioplasty. Biomedical Signal Processing and Control **11**, 97–106 (2014)
4. Bonomini, M., Arini, P., Gonzalez, G., et al.: The allometric model in chronic myocardial infarction. Theor Biol Med Model **9**, 15–22 (2012)
5. Bonomini, M., Ortega, D., Barja, L., Logarzo, E., Mangani, N., Paolucci, A.: Ecg parameters to predict left ventricular electrical delay. J of Electrocardiol **51**, 844–850 (2018)
6. Bonomini, M., Ortega, D., Barja, L., Mangani, N., Arini, P.: Depolarization spatial variance as a cardiac dyssynchrony descriptor. Biomedical Signal Processing and Control **49**, 540–545 (2019)
7. Bonomini, M., Villarroel-Abrego, H., Garillo, R.: Spatial variance in the 12-lead ecg and mechanical dyssynchrony. J Interv Card Electrophysiol **62**, 479–485 (2021)

8. Breithardt, O., Kühl, H., Stellbrink, C.: Acute effects of resynchronisation treatment on functional mitral regurgitation in dilated cardiomyopathy. Heart **88**, 440 (2002)
9. Cortez DL, S.T.: When deriving the spatial qrs-t angle from the 12-lead electrocardiogram, which transform is more frank: regression or inverse dower?) (2010), https://pubmed.ncbi.nlm.nih.gov/20466388/
10. Draper, B.W.H., Peffer, C.J., Stallmann, F.W., Littmann, D., Pipberger, H.V.: The corrected orthogonal electrocardiogram and vectorcardiogram in 510 normal men (frank lead system), http://ahajournals.org
11. Ferrandez, J.M., Liano, E., Bonomini, P., Martinez, J., Toledo, J., Fernandez, E.: A customizable multi-channel stimulator for cortical neuroprosthesis. In: 2007 29th Annual International Conference of the IEEE Engineering in Medicine and Biology Society. pp. 4707–4710 (2007). https://doi.org/10.1109/IEMBS.2007.4353390
12. Ferrandez, J., Alfaro, A., Bonomini, P., Tormos, J., Concepcion, L., Pelayo, F., Fernandez, E.: Brain plasticity: feasibility of a cortical visual prosthesis for the blind. In: Proceedings of the 25th Annual International Conference of the IEEE Engineering in Medicine and Biology Society (IEEE Cat. No.03CH37439). vol. 3, pp. 2027–2030 Vol.3 (2003). https://doi.org/10.1109/IEMBS.2003.1280133
13. Jan, C., Borleffs, W., Roderick, ., Scherptong, W.C., Man, .S.C., Welsenes, G.H.V., Bax, J.J., Erven, .L.V., Swenne, C.A., Schalij, M.J.: Predicting ventricular arrhythmias in patients with ischemic heart disease clinical application of the ecg-derived qrs-t angle (2009). https://doi.org/10.1161/CIRCEP.109.859108, http://ahajournals.org
14. Kardys, I., Kors, J.A., Meer, I.M.V.D., Hofman, A., Kuip, D.A.M.V.D., Witteman, J.C.M.: Spatial qrs-t angle predicts cardiac death in a general population (2003). https://doi.org/10.1016/S0195-668X(03)00203-3, https://academic.oup.com/eurheartj/article/24/14/1357/501772
15. Ledezma CA: WTdelineator (2021), https://github.com/caledezma/WTdelineator
16. Martínez, J.P., Almeida, R., Olmos, S., Rocha, A.P., Laguna, P.: A wavelet-based ECG delineatior: Evaluation on standard databases. IEEE Trans. on Biomed. Eng. **51**(4), 570–581 (2004)
17. Martín-Yebra, A., Martínez, J.: Automatic diagnosis of strict left bundle branch block using a wavelet-based approach. PLoS One **14**, e0212971 (2019)
18. Moss, A.J., Hall, W.J., Cannom, D.S., Klein, H., Brown, M.W., Daubert, J.P., Estes, N.M., Foster, E., Greenberg, H., Higgins, S.L., Pfeffer, M.A., Solomon, S.D., Wilber, D., Zareba, W.: Cardiac-resynchronization therapy for the prevention of heart-failure events. New England Journal of Medicine **361**(14), 1329–1338 (2009)
19. Oehler, A., Feldman, T., Henrikson, C.A., Tereshchenko, L.G.: Qrs-t angle: A review. Ann Noninvasive Electrocardiol **19**, 534–542 (2014). https://doi.org/10.1111/anec.12206
20. Ortega, D., Logarzo, E., Barja, L., Paolucci, A., Mangani, N., Mazzetti, E., Bonomini, M.P.: Novel implant technique for septal pacing. a noninvasive approach to nonselective his bundle pacing. Journal of Electrocardiology **63**, 35–40 (2020)
21. Ortega, D.F., Barja, L.D., Logarzo, E., Mangani, N., Paolucci, A., Bonomini, M.P.: Nonselective his bundle pacing with a biphasic waveform. enhancing septal resynchronization. Europace **20**, 816–822 (2018)
22. Telemetric, of Rocher Medical Center, H.E.W.U.: E-hol-03-0202-003., http://thew-project.org/Database/E-HOL-03-0202-003.html